Preprints of the 21st IFAC World Congress (Virtual)
Berlin, Germany, July 12-17, 2020

Curvature and Force Estimation for a Soft Finger using an EKF with Unknown Input Optimization

Junn Yong Loo [*,1], **Ze Yang Ding** [*,1], **Evan Davies** [*], **Surya Girinatha Nurzaman** [*], **Chee Pin Tan** [*,2]

[*] *School of Engineering and Advanced Engineering Platform, Monash University Malaysia, 47500 Selangor, Malaysia (e-mail: junn.loo/ze.ding/surya.nurzaman/tan.chee.pin/@monash.edu)*

Abstract: Sensory data such as bending curvature and contact force are essential for controlling soft robots. However, it is inconvenient to measure these variables because sensorizing soft robots is difficult due to their inherent softness. An attractive alternative is to use an observer/filter to estimate the variables that would have been measured by those sensors. Nevertheless, an observer/filter requires a model which can be analytically demanding for soft robots due to their high nonlinearity. In this paper, we propose an Unknown Input Extended Kalman Filter (UI-EKF) consisting of an EKF interconnected with a UI-optimizer to respectively estimate the state (curvature) and unknown input (contact force) for a pneumatic-based soft finger based on an identified nonlinear model. We also prove analytically that the estimation errors are bounded. Experimental results show that the UI-EKF can perform the estimation with high accuracy, even when the identified system model is not accurate and the sensor measurement is noisy. In other words, the proposed framework is able to estimate proprioceptive (internal) and exteroceptive (external) variables (curvature and contact force respectively) of the robot using a single sensor (flex), which is still an open problem in soft robotics.

Keywords: Extended Kalman filters; Unknown input estimation; Neural-network models; Stochastic systems; Lyapunov Stability; Robotics

1. INTRODUCTION

Inspired by the inherent softness and compliance found in biological organisms, soft robots are designed to have these characteristic for adaptive operation in unstructured environments (Nurzaman et al., 2014). For control purposes, soft robots should ideally have access to sensory data just like their rigid counterparts. For example, curvature angle is useful in describing the bending of soft actuators for feedback control (Webster and Jones, 2010). External force is also important because soft robots generally have to interact with objects and obstacles in real applications. However, integrating sensors in soft robots to measure these variables is not as straightforward as for their rigid counterparts (Rus and Tolley, 2015). For instance, attaching multiple load cells on a soft robot for force measurement introduces extra weight which could stiffen it, whilst cameras, which are used for measuring the curvature of a soft robot, are impractical to setup especially in unstructured environments. Due to this difficulty, many soft robots are still open-loop systems (Wang et al., 2017). To reduce the need of integrating sensors in soft robots, an alternative is to employ estimation methods.

A convenient estimation approach is using an empirical model identified by experimental data. For example, Elgeneidy et al. (2018) developed data-driven models using linear regression and neural networks to estimate the curvature angles of a pneumatic actuator. Thuruthel et al. (2019) trained a long short-term memory (LSTM) network as the kinematic and force model to estimate the tip position and contact force of their soft finger. However, these empirical methods heavily depend on sensor measurements which could be noisy, thereby reducing the estimation accuracy. Another estimation method is through optimization, for example Wang and Hirai (2017) estimated the grasping force of their soft robot by minimizing the discrepancy between the model estimates and sensor measurements. Recent work by Venkiteswaran et al. (2019) developed a pseudo-rigid body model with parameter optimization to estimate the forces applied on a magnetically-actuated manipulator. Nonetheless, the optimization accuracy is adversely affected by modelling error, which can be significant in soft robots due to their high nonlinearity. Hence, it can be seen that the estimation approaches in the aforementioned works are *open-loop*, and to get a good estimate would require accurate sensor measurements and a high-fidelity model, both of which are difficult or expensive to attain in soft robots. An observer/filter, that processes sensor measurements based on a model in *closed-loop*, could be a promising alternative to these methods.

⋆ This work was supported by the Ministry of Higher Education Malaysia under the Fundamental Grant Scheme (FRGS) grant no. FRGS/1/2016/TK03/MUSM/01/1.

[1] These authors contributed equally to this work.

[2] Corresponding author.

There are only few studies that utilize an observer/filter for state estimation in soft robots. A Luenberger observer was used to estimate the position and velocity using a reduced order steady-state model (Thieffry et al., 2019). Lunni et al. (2018) used an Adaptive Extended Kalman Filter on a simplified quasi-static model to estimate the angle of rotation at each flexural joint of a tendon-driven soft robot. Loo et al. (2019a,b) proposed an Extended Kalman Filter (EKF) to estimate states in the actuator and configuration space of both planar and non-planar pneumatic-based soft tentacles. However, none of these filter-based approaches estimated the contact force, which is an external signal (or unknown input). To the best of our knowledge, discrete-time filters by themselves cannot estimate unknown inputs. A possible solution is to integrate the filters with an additional component such as an optimizer for unknown input estimation. In the field of structural control for example, Huang et al. (2010); Liu et al. (2016) combined Kalman Filters with least square optimization to estimate unknown input in nonlinear systems, but only for a specific class of systems in which the measurement model must be a function of the unknown input.

In this paper, we present a general observer/filter-based framework for state and unknown input estimation of a pneumatic soft finger. Using a single flex sensor that can be conveniently embedded in the finger, we estimate the curvature angle and contact force, which are difficult to measure. Due to the complexities involved in analytical modelling of soft robots (Rus and Tolley, 2015), we employ system identification to model the soft finger, using a NARX model with wavelet network to represent its state dynamics, and nonlinear regression model to represent its output equation. The models that we use are a class of non-recurrent methods, that are less complex compared to recurrent network structure such as that in (Thuruthel et al., 2019). In the model, the curvature angle is formulated as an internal state because it relates to proprioception (produced and perceived within the soft finger), whereas the contact force, being an exteroceptive stimulus, is modelled as an unknown input. Based on the identified models, we propose an Unknown Input Extended Kalman Filter scheme (UI-EKF) consisting of an EKF interconnected with an UI-optimizer to estimate the curvature and contact force respectively. We also prove that the estimation errors are bounded. Experimental results show that the UI-EKF is capable of estimating the curvature and contact force to a high degree of accuracy. In the model that we identified, the unknown input (contact force) does not appear in the measurement equation, and hence the methods by Huang et al. (2010) and Liu et al. (2016) are not applicable to our system. In other words, we have demonstrated the ability of the framework in estimating both proprioceptive (internal) and exteroceptive (external) variables using a single sensor, which is still a significant challenge in soft robotics.

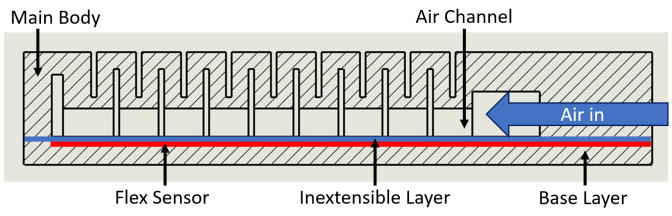

Fig. 1. Cross-sectional illustration of the PSF design.

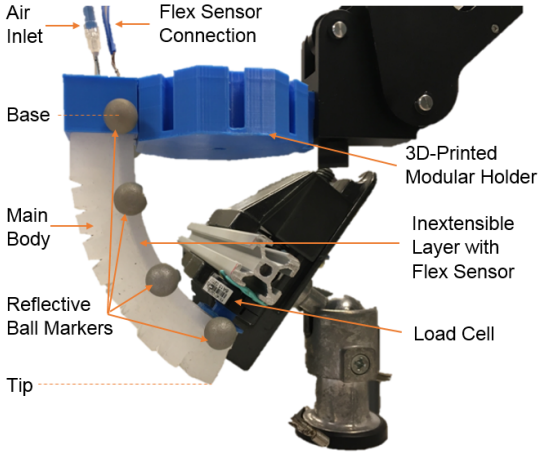

Fig. 2. Experimental setup of the soft finger (actuated).

This paper is organized as follows. Section 2 describes the soft robot fabrication method and experimental setup. Section 3 details the framework of the proposed UI-EKF. Results are presented and discussed in Section 4. Lastly, we conclude our work in Section 5.

2. MATERIALS

2.1 Fabrication of the Pneumatic Based Soft Robot

The soft robot used was a pneumatic-based soft finger (PSF). We casted silicone (EcoFlex 0050, Smooth-On Inc.) using 3D-printed molds to form the main body and a base layer. After that, we embedded a flex sensor (4.5 inches, SparkFun) in the base layer together with a piece of paper to make it inextensible. Then, the base layer and the main body were joined together with more silicone. Finally, we soldered the connections of the flex sensor and prodded the PSF with a sharp-end pneumatic pipe as air inlet. The cross-sectional view of the PSF is shown in Fig. 1.

2.2 Experimental Setup

Our pneumatic system consisted of a pneumatic supply connected in series to a pressure regulator followed by a solenoid valve (VQD1151U-5L, SMC Pneumatics), which was used to modulate the pressure by high-speed switching using PWM signals (Memarian et al., 2015). Finally, the modulated supply was connected to the PSF inlet and a pressure sensor (MPXH6400A, NXP) in parallel. The pressure inside the PSF was assumed to be the same as the measured pressure. We used a microcontroller (PSOC®5LP) to manipulate the duty cycle (control input) of the PWM signal that controls the solenoid valve. The amplitude and pulse width of the signals followed a pseudorandom sequence.

To capture the motion of the PSF, we attached it to a holder and placed reflective ball markers on its base, mid and tip position. During actuation, 3 cameras (OptiTrack Flex 13, NaturalPoint Inc.) continuously measured the coordinates of the markers to be used as ground-truth

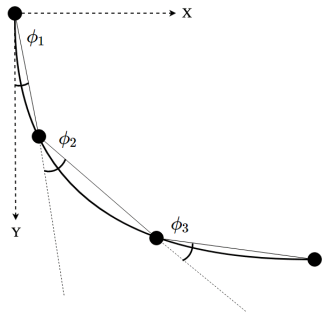

Fig. 3. Piece-wise constant curvature model of the PSF.

in the identification and estimation process. In addition, a sensing circuit was used to convert the the change in resistance of the embedded flex sensor to voltage readings. For tip contact force measurements, we used a load cell (FX1901, TE Connectivity) to obtain the ground-truth by positioning it near the PSF's tip. The experimental setup is shown in Fig. 2.

2.3 Data Collection

The sensors (for pressure, flex and force) were connected to the analog pins of an Arduino Mega 2560 board for data sampling whereas the markers' coordinates were provided by OptiTrack's Motive software. We collected the measurements at a rate of 11.5 Hz using MATLAB. 11 sets of 10-minute data and 4 sets of 5-minute data were collected as identification and validation data respectively. Each set corresponded to a different location of the load cell in front of the tip; this was to simulate the unstructuredness of real world environment in which the obstacles could be in any arbitrary location when in contact with the tip.

3. METHODS

3.1 Planar Bending Modelling

The motivation behind choosing curvature angle to characterize the PSF bending is the fact that the angle subtended by the bending arc of a single segment, θ_i is the total change in tangential direction along that arc as illustrated in (Loo et al., 2019a). Here we use a piece-wise constant curvature (PCC) analysis to calculate the angle ϕ_i between any two consecutive segments using method in (Wang and Hirai, 2017), given the nodal point coordinates as the measured markers' coordinates, as shown in Fig. 3. We also considered the case when the 2^{nd} and 3^{rd} markers

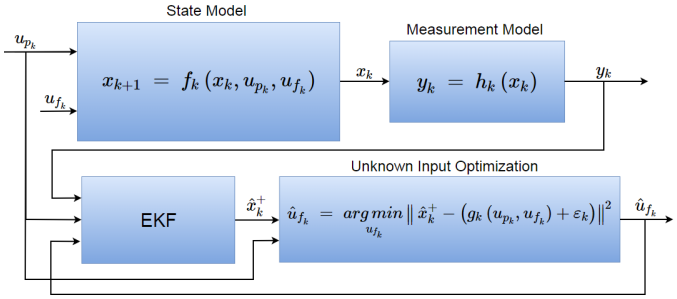

Fig. 4. Block diagram of pneumatic soft finger system and UI-EKF.

are to the left of the base marker by placing the origin at the most leftward marker and calculate ϕ_i as before so that the bending arc always extends out from the origin marker, parallel to Y axis. With that, we approximate the segmental curvature angle using the relationship $\theta_i = 2\,\phi_i$ (Webster and Jones, 2010). Finally, we quantify the curvature of the whole PSF as sum of the discrete segmental curvature angles, $\theta = \sum_{i=1}^{3} \theta_i$.

3.2 System Identification

The dynamics of the curvature angle that characterizes the bending of the soft finger can be represented using a general nonlinear *state model* and a nonlinear *measurement model* as follows

$$\dot{x} \;=\; \Phi(x, u_1, u_2) \quad , \quad y \;=\; \Gamma(x) \tag{1}$$

where x is the system state (curvature angle), u_1 is the known system input (PSF's internal pressure), u_2 is the unknown system input (tip contact force), y is the measurement output (flex sensor voltage).

Using the Forward-Euler scheme, we discretize the continuous models (1) by approximating the curvature angular velocity, $\dot{x}_k$ at each time step as

$$\dot{x}_k \;\approx\; \frac{x_{k+1} \;-\; x_k}{t_s} \tag{2}$$

where t_s is the sampling time step, to get the following discrete-time models:

$$x_{k+1} \;=\; x_k \;+\; \Phi(x_k, u_{1_k}, u_{2_k})\, t_s \;=\; f(x_k, u_{1_k}, u_{2_k}) \tag{3}$$

$$y_k \;=\; h(x_k) \tag{4}$$

where $f(\cdot)$ is the system difference equation function and $h(\cdot)$ is the discretized version of $\Gamma(\cdot)$. Fig. 4 illustrates this configuration.

Since the soft robot is slowly-actuated, we can disregard its dynamics, and assume $\dot{x}_k \approx 0$, i.e.

$$\Phi(x_k, u_{1_k}, u_{2_k}) \;\approx\; 0 \tag{5}$$

from which we can get the following quasi-static model:

$$x_k \;=\; g_k(\, u_{1_k}, \hat{u}_{2_k}\,) \tag{6}$$

Following our previous approach (Loo et al., 2019a), the state model is identified as a NARX model using a wavelet network with the modification of $\boldsymbol{x}_r \;=\; [x_k \; u_{p_k} \; u_{f_k}]$ as the regressor input. Similarly, the measurement model is identified as a fourth order polynomial function using polynomial regression.

3.3 Unknown Input Extended Kalman Filter

Consider a nonlinear discrete system with additive noises, represented by state and measurement models as follows

$$x_{k+1} \;=\; f(x_k, u_{1_k}, u_{2_k}) + \mathrm{G}_k w_k \tag{7}$$

$$y_k \;=\; h(x_k) + \mathrm{D}_k v_k \tag{8}$$

Here, w_k and v_k are modelling error and measurement noise of (3),(4), both assumed to have zero mean and unit covariance. In this paper, we introduce a novel observation-based filter structure termed as UI-EKF (Fig. 4), in which the conventional EKF is interconnected with a least square optimization scheme to simultaneously estimate the state (curvature) and unknown input (contact force) of

a nonlinear stochastic system. The formulations are as follows:

EKF Predict phase:

$$\hat{x}^-_{k+1} \;=\; f(\hat{x}^+_k, u_{1_k}, \hat{u}_{2_k}) \tag{9}$$
$$\mathrm{P}^-_{k+1} \;=\; \mathrm{F}_k\,\mathrm{P}^+_k\,\mathrm{F}^\top_k \;+\; \mathrm{Q}_k \tag{10}$$

where

$$\mathrm{F}_k \;=\; \mathrm{A}_k + \eta \mathrm{B}_k \tag{11}$$

EKF Correct phase:

$$\mathrm{K}_{k+1} \;=\; \mathrm{P}^-_{k+1}\mathrm{C}^\top_{k+1}\big[\mathrm{C}_{k+1}\mathrm{P}^-_{k+1}\mathrm{C}^\top_{k+1} + \mathrm{R}_{k+1}\big]^{-1} \tag{12}$$
$$\hat{x}^+_{k+1} \;=\; \hat{x}^-_{k+1} + \mathrm{K}_{k+1}\big(\, y_{k+1} - h(\hat{x}^-_{k+1})\,\big) \tag{13}$$
$$\mathrm{P}^+_{k+1} \;=\; \big[\mathrm{I} - \mathrm{K}_{k+1}\mathrm{C}_{k+1}\big]\mathrm{P}^-_{k+1} \tag{14}$$

where A_k, B_k and C_k are the state, input and measurement Jacobians respectively, obtained as

$$\mathrm{A}_k = \left.\frac{\partial f}{\partial x}\right|_{\hat{x}^+_k, u_{1_k}, \hat{u}_{2_k}} \quad \mathrm{B}_k = \left.\frac{\partial f}{\partial u_2}\right|_{\hat{x}^+_k, u_{1_k}, \hat{u}_{2_k}} \quad \mathrm{C}_{k+1} = \left.\frac{\partial h}{\partial x}\right|_{\hat{x}^-_{k+1}} \tag{15}$$

Unknown Input Optimization:

$$\hat{u}_{2_k} \;=\; \underset{u_{2_k}}{\arg\min} \left\| \hat{x}^+_k - g(\, u_{1_k}, u_{2_k}\,) \right\|^2 \tag{16}$$
$$:=\; \psi(\, \hat{x}^+_k, u_{1_k}, \varepsilon_k\,) \tag{17}$$

where ε_k is the modelling error of (6). In (16), we estimate the unknown input, $\hat{u}_{2_k}$ via a nonlinear Least Square Optimization as shown.

This quasi-static model (6) is identified using a 1-hidden layer, Rectified Linear Unit (ReLU) activated neural network. We used the ReLU activation to conserve the convexity of the function thereby preventing the optimization solution from being a local minima. A quasi-static approximation is valid since there is no rapid dynamics in our pneumatic soft finger. For fast-actuated system, the dynamic model (7) can be used for unknown input optimization (16) instead.

Define the estimation errors to be

$$e_k = x_k - \hat{x}^+_k \;,\; z_k = x_k - \hat{x}^-_k \;,\; \xi_k = u_{2_k} - \hat{u}_{2_k} \tag{18}$$

Then

$$\xi_k = \psi(x_k, u_{1_k}, \varepsilon_k) - \psi(\hat{x}^+_k, u_{1_k}, \varepsilon_k) \;:=\; \Psi(x_k, \hat{x}^+_k) \tag{19}$$

The Taylor's expansion of $f(\cdot)$ at $\hat{x}^+_k$ and $h \circ f(\cdot)$ at $\hat{x}^-_{k+1}$ are

$$\begin{aligned}
&f(\, x_k, u_{1_k}, u_{2_k}\,) - f(\, \hat{x}^+_k, u_{1_k}, \hat{u}_{2_k}\,) \\
&= \mathrm{J}_k\zeta_k + \varphi(\, x_k, \hat{x}^+_k, u_{2_k}, \hat{u}_{2_k}\,) \\
&\quad h\big(\, f(\, x_k, u_{1_k}, u_{2_k}\,) + \mathrm{G}_k w_k\,\big) - h\big(\, f(\, \hat{x}^+_k, u_{1_k}, \hat{u}_{2_k}\,)\,\big) \\
&= \mathrm{C}_{k+1}\big(\, \mathrm{J}_k\zeta_k + \varphi(\, x_k, \hat{x}^+_k, u_{2_k}, \hat{u}_{2_k}\,) + \mathrm{G}_k w_k\,\big) \\
&\quad + \chi(\, x_{k+1}, \hat{x}^-_{k+1}\,)
\end{aligned} \tag{20}$$

where we have used chain rule for $h \circ f(\cdot)$ and

$$\mathrm{J}_k = [\mathrm{A}_k \;\; \mathrm{B}_k]\,, \quad \zeta_k = \begin{bmatrix} e_k \\ \xi_k \end{bmatrix} \tag{21}$$

Introduce the *a priori* estimation error as

$$\begin{aligned}
z_{k+1} \;&=\; x_{k+1} - \hat{x}^-_{k+1} \\
&= f(\, x_k, u_{1_k}, u_{2_k}\,) - f(\, \hat{x}^+_k, u_{1_k}, \hat{u}_{2_k}\,) + \mathrm{G}_k w_k \\
&= \mathrm{J}_k\zeta_k + \varphi(\cdot) + \mathrm{G}_k w_k
\end{aligned} \tag{22}$$

Introduce the *a posteriori* estimation error as

$$\begin{aligned}
e_{k+1} \;&=\; x_{k+1} - \hat{x}^+_{k+1} \\
&= x_{k+1} - \Big(\, \hat{x}^-_{k+1} + \mathrm{K}_{k+1}\big(\, y_{k+1} - h(\hat{x}^-_{k+1})\,\big)\,\Big) \\
&= f(\, x_k, u_{1_k}, u_{2_k}\,) + \mathrm{G}_k w_k - f(\, \hat{x}^+_k, u_{1_k}, \hat{u}_{2_k}\,) \\
&\quad - \mathrm{K}_{k+1}\Big(\, h\big(\, f(\, x_k, u_{1_k}, u_{2_k}\,) + \mathrm{G}_k w_k\,\big) + \mathrm{D}_{k+1} v_{k+1} \\
&\quad - h\big(\, f(\, \hat{x}^+_k, u_{1_k}, \hat{u}_{2_k}\,)\,\big)\,\Big) \\
&= \mathrm{J}_k\zeta_k - \mathrm{K}_{k+1}\mathrm{C}_{k+1}\mathrm{J}_k\zeta_k + r_k + s_k \\
&= \big[\mathrm{I} - \mathrm{K}_{k+1}\mathrm{C}_{k+1}\big]\,\mathrm{J}_k\zeta_k + r_k + s_k
\end{aligned} \tag{23}$$

where

$$r_k \;=\; \big[\mathrm{I} - \mathrm{K}_{k+1}\mathrm{C}_{k+1}\big]\,\varphi(\cdot) - \mathrm{K}_{k+1}\,\chi(\cdot) \tag{24}$$
$$s_k \;=\; \big[\mathrm{I} - \mathrm{K}_{k+1}\mathrm{C}_{k+1}\big]\,\mathrm{G}_k w_k - \mathrm{K}_{k+1}\mathrm{D}_{k+1} v_{k+1} \tag{25}$$

Here, we make the following global boundedness assumptions

$$\big\|\mathrm{A}_k\big\| \;\le\; \bar{a} \quad , \quad \big\|\mathrm{B}_k\big\| \;\le\; \bar{b} \quad , \quad \big\|\mathrm{C}_k\big\| \;\le\; \bar{c} \tag{26}$$
$$\underline{q}\mathrm{I} \;\le\; \mathrm{Q}_k \;\le\; \bar{q}\mathrm{I} \quad , \quad \underline{r}\mathrm{I} \;\le\; \mathrm{R}_k \;\le\; \bar{r}\mathrm{I} \tag{27}$$
$$\underline{p}\mathrm{I} \;\le\; \mathrm{P}^+_k \;\le\; \bar{p}\mathrm{I} \tag{28}$$

and the following global Lipchitz assumptions:

$$\|\xi_k\| \;=\; \big\|\Psi(\, x_k, \hat{x}^+_k\,)\big\| \;\le\; \eta\|e_k\| \tag{29}$$
$$\begin{aligned}
&\big\|\varphi(\, x_k, \hat{x}^+_k, u_{2_k}, \hat{u}_{2_k}\,)\big\| \;\le\; \kappa_\varphi\|\zeta_k\|^2 \\
&\quad\le\; \kappa_\varphi(\|e_k\|^2 + \|\xi_k\|^2) \;\le\; \kappa_\varphi(1+\eta^2)\,\|e_k\|^2
\end{aligned} \tag{30}$$
$$\big\|\chi(\, x_{k+1}, \hat{x}^-_{k+1}\,)\big\| \;\le\; \kappa_\chi\|z_{k+1}\|^2 \tag{31}$$

Lemma 1. Under the assumptions (26)-(28), there exists a positive real number $\beta < 1$ such that $\Pi_k = \mathrm{P}^{+^{-1}}_k$ satisfies

$$\mathrm{F}^\top_k\big[\mathrm{I} - \mathrm{K}_{k+1}\mathrm{C}_{k+1}\big]^\top\Pi_{k+1}\big[\mathrm{I} - \mathrm{K}_{k+1}\mathrm{C}_{k+1}\big]\mathrm{F}_k \;\le\; \Pi_k(1-\beta)$$

Proof. See Appendix A.1.

Lemma 2. Under the Lipchitz assumptions (29)-(31) and let r_k be given by (24), there exist positive real numbers κ_{nonl_1}, κ_{nonl_2} and κ_{nonl_w} such that $\Pi_k = \mathrm{P}^{+^{-1}}_k$ satisfies

$$\begin{aligned}
&\mathbb{E}\Big[r^\top_k\Pi_{k+1}\Big(2\big[\mathrm{I} - \mathrm{K}_{k+1}\mathrm{C}_{k+1}\big]\,\mathrm{J}_k\zeta_k + r_k\Big)\Big] \\
&\le \kappa_{nonl_1}(\|e_k\|) + \kappa_{nonl_2}(\|e_k\|)\delta_w + \kappa_{nonl_w}\delta^2_w
\end{aligned}$$

Proof. See Appendix A.2.

Lemma 3. Let s_k be given by (25), there exist positive real numbers κ_{noise_w} and κ_{noise_v} such that $\Pi_k = \mathrm{P}^{+^{-1}}_k$ satisfies

$$\mathbb{E}\big[s^\top_k\Pi_{k+1}s_k\big] \;\le\; \kappa_{noise_w}\delta_w + \kappa_{noise_v}\delta_v$$

Proof. See Appendix A.3.

Proposition 1. Under assumptions (26)-(31), the UI-EKF described by (9)-(16) is able to estimate the state and unknown input of system (7)-(8) with errors exponentially

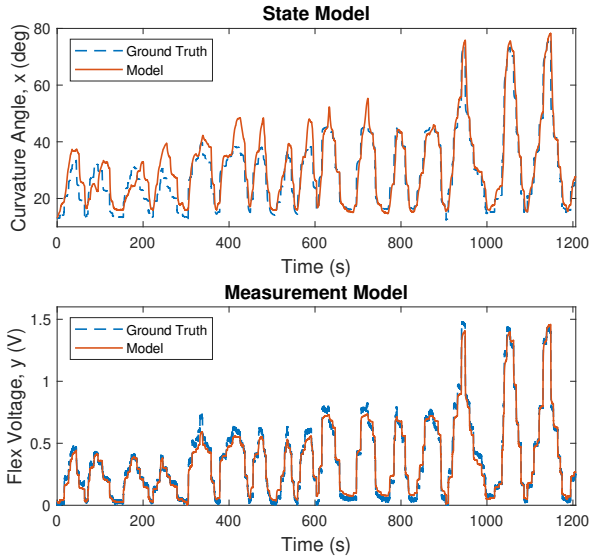

Fig. 5. Validation of system model (top) and measurement model (bottom) identification.

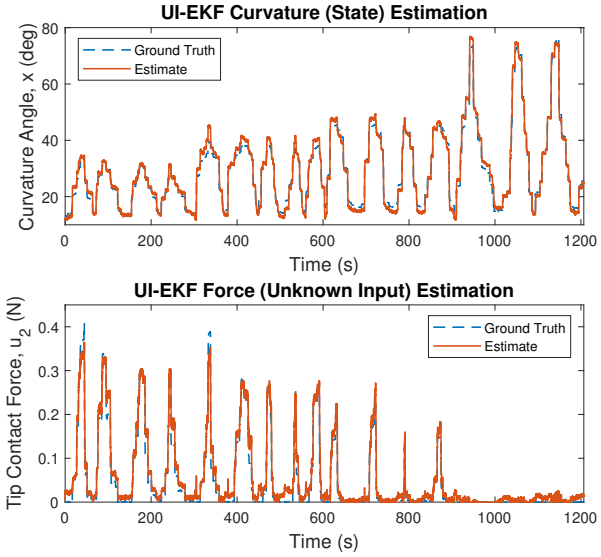

Fig. 6. Result of curvature (top) and contact force (bottom) estimation.

bounded in mean square with probability one, provided that the initial state error is small i.e.

$$\|e_0\| \leq \epsilon \tag{32}$$

and the model error and sensor noise are bounded i.e.

$$\mathrm{G}_k\mathrm{G}_k^\top \leq \delta_w \mathrm{I} \quad , \quad \mathrm{D}_k\mathrm{D}_k^\top \leq \delta_v \mathrm{I} \tag{33}$$

Proof. See Appendix A.4.

Remark: Assuming that our identified system (3),(4) is locally observable (i.e. two distinct states, x^1, x^2 are U-distinguishable for every admissible system input, u, implying that the nonlinear observability rank condition is satisfied) (Hermann and Krener, 1977) and their nonlinear functions, $f(\cdot), h(\cdot)$ are twice differentiable, then from *Lemma 4.1* and *Lemma 4.2* in (Reif et al., 1999), $\mathrm{A}_k, \mathrm{C}_k$ in (15) satisfy the uniform observability condition, thus condition (28) is valid if the noise covariances are bounded i.e. (27) holds. Lipchitz assumptions (29) generally holds if the objective function in (16) is convex and the model error, ε of (6) is small. According to (Reif et al., 1999, *Proof of Theorem 4.1*), $\kappa_\varphi, \kappa_\chi$ in (30), (31) are given by the spectral norm of the respective Hessian matrices of $f(\cdot), h(\cdot)$.

In practice, we use $\mathrm{P}_{k+1}^- = \mathrm{A}_k\,\mathrm{P}_k^+\,\mathrm{A}_k^\top + \mathrm{Q}_k$ instead of (10) for estimate covariance propagation in EKF while setting a higher Q_k to compensate for the term $\eta^2\mathrm{B}_k\mathrm{P}_k^+\mathrm{B}_k^\top$ at each time step, so that we circumvent the difficulty of finding the global Lipchitz constant, η in (29).

4. RESULTS & DISCUSSIONS

4.1 System Identification

With the identification data, the state model $f(\cdot)$ is identified as a wavelet-based NARX model using x_k (curvature), u_{1_k} (pressure) and u_{2_k} (force) as inputs and x_{k+1} as output, whereas the measurement model $h(\cdot)$ uses a 4^{th} order polynomial to fit x_k and y_k (flex voltage) as input and output respectively. The model is then tested against the validation data, and its normalized root-mean-squared error (NRMSE) is used to indicate the quality of fit. Fig. 5 shows the validation results of the state model (top) and measurement model (bottom), with a NRMSE of 7.47% and 2.72% respectively. The validation results also show that both the open-loop models (state and measurement) are able to capture the soft robot's dynamics well and also estimate the curvature angles, but only to a certain accuracy with the respective margin of errors. In addition, the identified model requires the knowledge of contact force for estimation, and it cannot be used for real-time testing as contact force is an unknown quantity.

4.2 State and Unknown Input Estimation

Using the identified models, the UI-EKF closed-loop framework is employed to estimate both the curvature and contact force. Fig. 6 (top) shows the curvature estimation result with a much-improved NRMSE of 2.94% compared to the open-loop estimation (Fig. 5-top). Even without the knowledge of contact force. the EKF is able to estimate the curvature with a high accuracy. In addition, the EKF, being a filter, reduces the effect of noise from the measurement output onto the estimated state.

Fig. 6 (bottom) shows the result for contact force estimation, with a NRMSE of 4.05%. This indicates that our proposed UI-EKF framework is successful in estimating not only the state, but also the unknown input. Furthermore, the force estimate is much less affected by measurement noise because it is obtained by the UI optimizer using the filtered curvature angle.

5. CONCLUSION

In this work, we present a novel Unknown Input Extended Kalman Filter (UI-EKF) to estimate the state (curvature) and unknown input (contact force) for a pneumatic soft finger based on an identified nonlinear model, and measurements of pressure and flex voltage (which are more convenient to obtain in our setting). We also prove that the estimation errors are bounded. The results show that

the estimates from the UI-EKF are very accurate. Finally, the paper has also shown that the proposed framework can estimate both proprioceptive (internal) and exteroceptive (external) variables using only a single sensor, resolving a significant challenge in soft robotics. Future work includes estimation in more complex soft robotic systems.

REFERENCES

Elgeneidy, K., Lohse, N., and Jackson, M. (2018). Bending angle prediction and control of soft pneumatic actuators with embedded flex sensors–a data-driven approach. *Mechatronics*, 50, 234–247.

Hermann, R. and Krener, A. (1977). Nonlinear controllability and observability. *IEEE Trans. Autom. Control*, 22(5), 728–740.

Huang, H., Yang, J.N., and Zhou, L. (2010). Adaptive quadratic sum-squares error with unknown inputs for damage identification of structures. *Structural Control and Health Monitoring*, 17(4), 404–426.

Liu, L., Su, Y., Zhu, J., and Lei, Y. (2016). Data fusion based ekf-ui for real-time simultaneous identification of structural systems and unknown external inputs. *Measurement*, 88, 456 – 467.

Loo, J.Y., Kong, K.C., Tan, C.P., and Nurzaman, S.G. (2019a). Non-linear system identification and state estimation in a pneumatic based soft continuum robot. In *2019 CCTA*.

Loo, J.Y., Tan, C.P., and Nurzaman, S.G. (2019b). H-infinity based extended kalman filter for state estimation in highly non-linear soft robotic system. In *2019 ACC*, 5154–5160. IEEE.

Lunni, D., Giordano, G., Sinibaldi, E., Cianchetti, M., and Mazzolai, B. (2018). Shape estimation based on kalman filtering: Towards fully soft proprioception. In *2018 RoboSoft*, 541–546. IEEE.

Memarian, M., Gorbet, R., and Kulić, D. (2015). Control of soft pneumatic finger-like actuators for affective motion generation. In *2015 IROS*, 1691–1697. IEEE.

Nurzaman, S.G., Iida, F., Margheri, L., and Laschi, C. (2014). Soft robotics on the move: Scientific networks, activities, and future challenges. *Soft Rob.*, 1(2), 154–158.

Reif, K., Gunther, S., Yaz, E., and Unbehauen, R. (1999). Stochastic stability of the discrete-time extended kalman filter. *IEEE Trans. Autom. Control*, 44(4), 714–728.

Rus, D. and Tolley, M.T. (2015). Design, fabrication and control of soft robots. *Nature*, 521(7553), 467.

Thieffry, M., Kruszewski, A., Duriez, C., and Guerra, T. (2019). Control design for soft robots based on reduced-order model. *IEEE Robot. Autom. Lett.*, 4(1), 25–32.

Thuruthel, T.G., Shih, B., Laschi, C., and Tolley, M.T. (2019). Soft robot perception using embedded soft sensors and recurrent neural networks. *Science Robotics*, 4(26), eaav1488.

Venkiteswaran, V.K., Sikorski, J., and Misra, S. (2019). Shape and contact force estimation of continuum manipulators using pseudo rigid body models. *Mech. Mach. Theory*, 139, 34–45.

Wang, L., Nurzaman, S.G., Iida, F., et al. (2017). Soft-material robotics. *Foundations and Trends® in Robotics*, 5(3), 191–259.

Wang, Z. and Hirai, S. (2017). Soft gripper dynamics using a line-segment model with an optimization-based parameter identification method. *IEEE Robot. Autom. Lett.*, 2(2), 624–631.

Webster, R.J. and Jones, B.A. (2010). Design and kinematic modeling of constant curvature continuum robots: A review. *The International Journal of Robotics Research*, 29(13), 1661–1683.

Appendix A. STABILITY PROOFS

The proofs follow closely the results of (Reif et al., 1999) who considered *a priori* estimation of a one-step EKF; in this paper, we also include unknown input estimation by considering the conventional two-step EKF in cascade with an unknown input optimization and prove for bounded error in both *a posteriori* state and unknown input estimates. Hence, *Lemma 1*, *Lemma 2*, *Lemma 3* and *Proposition 1* follow from *Lemma 3.1*, *Lemma 3.2*, *Lemma 3.3* and *Theorem 3.1* in (Reif et al., 1999), but with the necessary modifications.

A.1 Proof of Lemma 1. The posteriori estimate covariance propagation equation in (14) can be reformulated into

$$\begin{aligned}
\mathrm{P}_{k+1}^{+} &= \big[\mathrm{I}-\mathrm{K}_{k+1}\mathrm{C}_{k+1}\big]\mathrm{P}_{k+1}^{-}\big[\mathrm{I}-\mathrm{K}_{k+1}\mathrm{C}_{k+1}\big]^{\top} \\
&\quad + \mathrm{K}_{k+1}\mathrm{R}_{k+1}\mathrm{K}_{k+1}^{\top} \\
&= \big[\mathrm{I}-\mathrm{K}_{k+1}\mathrm{C}_{k+1}\big]\big[\mathrm{F}_k\mathrm{P}_k^{+}\mathrm{F}_k^{\top}+\mathrm{Q}_k\big]\big[\mathrm{I}-\mathrm{K}_{k+1}\mathrm{C}_{k+1}\big]^{\top} \\
&\quad + \mathrm{K}_{k+1}\mathrm{R}_{k+1}\mathrm{K}_{k+1}^{\top} \\
&= \big[\mathrm{I}-\mathrm{K}_{k+1}\mathrm{C}_{k+1}\big]\mathrm{F}_k\Big[\mathrm{P}_k^{+}+\mathrm{F}_k^{-1}\mathrm{Q}_k\mathrm{F}_k^{-\top} \\
&\quad + \mathrm{F}_k^{-1}\big[\mathrm{I}-\mathrm{K}_{k+1}\mathrm{C}_{k+1}\big]^{-1}\mathrm{K}_{k+1}\mathrm{R}_{k+1}\mathrm{K}_{k+1}^{\top} \\
&\quad \times \big[\mathrm{I}-\mathrm{K}_{k+1}\mathrm{C}_{k+1}\big]^{-\top}\mathrm{F}_k^{-\top}\Big]\mathrm{F}_k^{\top}\big[\mathrm{I}-\mathrm{K}_{k+1}\mathrm{C}_{k+1}\big]^{\top} \\
&\geq \big[\mathrm{I}-\mathrm{K}_{k+1}\mathrm{C}_{k+1}\big]\mathrm{F}_k\times \\
&\quad \mathrm{P}_k^{+}\bigg(1+\frac{1}{\overline{p}(\overline{a}+\eta\overline{b})^2}\Big(\underline{q}+\frac{\underline{p}^2\underline{c}^2}{\overline{r}\big(1+\overline{pc}^2\frac{1}{\underline{r}}\big)^2}\Big)\bigg) \\
&\quad \times \mathrm{F}_k^{\top}\big[\mathrm{I}-\mathrm{K}_{k+1}\mathrm{C}_{k+1}\big]^{\top}
\end{aligned} \tag{A.1}$$

where we used the fact that (12) can be rewritten into

$$\mathrm{K}_k \;=\; \mathrm{P}_k^{+}\mathrm{C}_k^{\top}\mathrm{R}_k^{-1}, \quad \underline{pc}\frac{1}{\overline{r}} \;\leq\; \|\mathrm{K}_k\| \;\leq\; \overline{pc}\frac{1}{\underline{r}} \tag{A.2}$$

Taking the inverse on both sides of (A.1),

$$\begin{aligned}
&{\mathrm{P}_{k+1}^{+}}^{-1} \;\leq\; \big[\mathrm{I}-\mathrm{K}_{k+1}\mathrm{C}_{k+1}\big]^{-\top}\mathrm{F}_k^{-\top}\times \\
&\mathrm{P}_k^{+-1}\bigg(1+\frac{1}{\overline{p}(\overline{a}+\eta\overline{b})^2}\Big(\underline{q}+\frac{\underline{p}^2\underline{c}^2}{\overline{r}\big(1+\overline{pc}^2\frac{1}{\underline{r}}\big)^2}\Big)\bigg)\times \\
&\mathrm{F}_k^{-1}\big[\mathrm{I}-\mathrm{K}_{k+1}\mathrm{C}_{k+1}\big]^{-1} \\
&\mathrm{F}_k^{\top}\big[\mathrm{I}-\mathrm{K}_{k+1}\mathrm{C}_{k+1}\big]^{\top}{\mathrm{P}_{k+1}^{+}}^{-1}\big[\mathrm{I}-\mathrm{K}_{k+1}\mathrm{C}_{k+1}\big]\mathrm{F}_k \\
&\quad \leq\; \mathrm{P}_k^{+-1}\bigg(1+\frac{1}{\overline{p}(\overline{a}+\eta\overline{b})^2}\Big(\underline{q}+\frac{\underline{p}^2\underline{c}^2}{\overline{r}\big(1+\overline{pc}^2\frac{1}{\underline{r}}\big)^2}\Big)\bigg)^{-1}
\end{aligned}$$

By letting $\Pi_k = \mathrm{P}_k^{+-1}$,

$$\begin{aligned}&\mathrm{F}_k^\top\big[\mathrm{I}-\mathrm{K}_{k+1}\mathrm{C}_{k+1}\big]^\top\Pi_{k+1}\big[\mathrm{I}-\mathrm{K}_{k+1}\mathrm{C}_{k+1}\big]\mathrm{F}_k\\ &\le \Pi_k\frac{1}{1+\frac{1}{\overline{p}(\overline{a}+\eta\overline{b})^2}\Big(\underline{q}+\frac{\underline{p}^2\underline{c}^2}{\overline{r}\big(1+\overline{pc}^2\frac{1}{\underline{r}}\big)^2}\Big)} \;=\; \Pi_k\,(1-\beta)\end{aligned}$$

A.2 Proof of Lemma 2. From (24),(30),(31),(22) we have

$$\begin{aligned}&\|r_k\| \;\le\; \big\|[\mathrm{I}-\mathrm{K}_{k+1}\mathrm{C}_{k+1}]\varphi(\cdot)\big\|+\big\|\mathrm{K}_{k+1}\chi(\cdot)\big\|\\ &\le (1+\overline{pc}^2\frac{1}{\underline{r}})\kappa_\varphi\|\zeta_k\|^2+\overline{pc}\frac{1}{\underline{r}}\kappa_\chi\|\mathrm{J}_k\zeta_k+\varphi(\cdot)+\mathrm{G}_kw_k\|^2\\ &\le \Big(1+\overline{pc}^2\frac{1}{\underline{r}}\kappa_\varphi+\overline{pc}\frac{1}{\underline{r}}\kappa_\chi(\overline{a}+\eta\overline{b})^2\Big)\|\zeta_k\|^2\\ &\quad+\overline{pc}\frac{1}{\underline{r}}\kappa_\chi\kappa_\varphi^2\|\zeta_k\|^4+\overline{pc}\frac{1}{\underline{r}}\kappa_\chi\|\mathrm{G}_kw_k\|^2\\ &\le \kappa_1'(1+\eta^2)\,\|e_k\|^2+\kappa_2'(1+\eta^4)\,\|e_k\|^4+\kappa_3\|\mathrm{G}_kw_k\|^2\\ &= \kappa_1\|e_k\|^2+\kappa_2\|e_k\|^4+\kappa_3\|\mathrm{G}_kw_k\|^2\end{aligned}$$

where we have used the facts that from (21) and (29), $\|\mathrm{J}_k\zeta_k\| \le (\|\mathrm{A}_k\|+\eta\|\mathrm{B}_k\|)\|e_k\|$. Given (33) holds and the fact that w_k is white, we have

$$\begin{aligned}&\mathbb{E}\Big[r_k^\top\Pi_{k+1}\Big(2\big[\mathrm{I}-\mathrm{K}_{k+1}\mathrm{C}_{k+1}\big]\,\mathrm{J}_k\zeta_k+r_k\Big)\Big]\\ &\le \mathbb{E}\Big[\kappa_1\|e_k\|^2+\kappa_2\|e_k\|^4+\kappa_3\|\mathrm{G}_kw_k\|^2\times\\ &\quad\frac{1}{\underline{p}}\Big(2\big(1+\overline{pc}^2\frac{1}{\underline{r}}\big)(\overline{a}+\eta\overline{b})\|e_k\|\\ &\quad+\kappa_1\|e_k\|^2+\kappa_2\|e_k\|^4+\kappa_3\|\mathrm{G}_kw_k\|^2\Big)\Big]\\ &\le \kappa_{nonl_1}(\|e_k\|)+\kappa_{nonl_2}(\|e_k\|)\,\mathrm{tr}\Big(\mathrm{G}_k\mathbb{E}\big[w_kw_k^\top\big]\mathrm{G}_k^\top\Big)\\ &\quad+\kappa_{nonl_w}\,\mathrm{tr}\Big(\mathrm{G}_k\mathbb{E}\big[w_kw_k^\top\big]\mathrm{G}_k^\top\Big)^2\\ &= \kappa_{nonl_1}(\|e_k\|)+\kappa_{nonl_2}(\|e_k\|)\delta_w+\kappa_{nonl_w}\delta_w^2\end{aligned}$$

where $\kappa_{nonl_1}(\cdot)$ and $\kappa_{nonl_2}(\cdot)$ are polynomial functions of $\|e_k\|$.

We also used the matrix identity for trace operation $\mathrm{tr}(\mathrm{AB})=\mathrm{tr}(\mathrm{BA})$, and the fact that

$$\mathrm{tr}\,\big(\mathrm{G}_k\mathrm{G}_k^\top\big) \;\le\; g\delta_w \quad,\quad \mathrm{tr}\,\big(\mathrm{D}_k\mathrm{D}_k^\top\big) \;\le\; d\delta_v \tag{A.3}$$

where g and d are the number of rows of G_k and D_k. Note that taking the trace of a scalar does not change its value.

A.3 Proof of Lemma 3. Taking the expectation of $s_k^\top\Pi_{k+1}s_k$, we get

$$\begin{aligned}&\mathbb{E}\big[s_k^\top\Pi_{k+1}s_k\big]\\ &=\mathbb{E}\Big[w_k^\top\mathrm{G}_k^\top\big[\mathrm{I}-\mathrm{K}_{k+1}\mathrm{C}_{k+1}\big]^\top\Pi_{k+1}\big[\mathrm{I}-\mathrm{K}_{k+1}\mathrm{C}_{k+1}\big]\mathrm{G}_kw_k\\ &\quad+v_{k+1}^\top\mathrm{D}_{k+1}^\top\mathrm{K}_{k+1}^\top\Pi_{k+1}\mathrm{K}_{k+1}\mathrm{D}_{k+1}v_{k+1}\Big]\end{aligned}$$

where the cross terms of w_k and v_k vanished since they are uncorrelated. With the fact that both w_k and v_k are white , we have

$$\begin{aligned}&\mathbb{E}\big[s_k^\top\Pi_{k+1}s_k\big] \;\le\; \frac{1}{\underline{p}}\big(1+\frac{\overline{pc}^2}{\underline{r}}\big)^2\,\mathrm{tr}\,\Big(\mathrm{G}_k\mathbb{E}\big[w_kw_k^\top\big]\mathrm{G}_k^\top\Big)\\ &\quad+\frac{\overline{p}^2\overline{c}^2}{\underline{p}\underline{r}^2}\,\mathrm{tr}\,\Big(\mathrm{D}_{k+1}\mathbb{E}\big[v_{k+1}v_{k+1}^\top\big]\mathrm{D}_{k+1}^\top\Big)\\ &=\frac{1}{\underline{p}}\big(1+\frac{\overline{pc}^2}{\underline{r}}\big)^2+\frac{\overline{p}^2\overline{c}^2}{\underline{p}\underline{r}^2}\,\mathrm{tr}\,\big(\mathrm{D}_{k+1}\mathrm{D}_{k+1}^\top\big)\\ &\le\frac{g}{\underline{p}}\big(1+\frac{\overline{pc}^2}{\underline{r}}\big)^2\delta_w+\frac{d\overline{p}^2\overline{c}^2}{\underline{p}\underline{r}^2}\delta_v \;=\; \kappa_{noise_w}\delta_w+\kappa_{noise_v}\delta_v\end{aligned}$$

A.4 Proof of Proposition 1. Choose a Lyapunov function $V_k(e_k) \;=\; e_k^\top\Pi_ke_k$, where $\Pi_k=\mathrm{P}_k^{+^{-1}}$. From (28) we have

$$\frac{1}{\overline{p}}\|e_k\|^2 \;\le\; V_k(e_k) \;\le\; \frac{1}{\underline{p}}\|e_k\|^2 \tag{A.4}$$

Then, from (23), we have

$$\begin{aligned}&V_{k+1}(e_{k+1}) \;=\; e_{k+1}^\top\Pi_{k+1}e_{k+1}\\ &=\Big[\big[\mathrm{I}-\mathrm{K}_{k+1}\mathrm{C}_{k+1}\big]\,\mathrm{J}_k\zeta_k+r_k+s_k\Big]^\top\times\\ &\quad\Pi_{k+1}\Big[\big[\mathrm{I}-\mathrm{K}_{k+1}\mathrm{C}_{k+1}\big]\,\mathrm{J}_k\zeta_k+r_k+s_k\Big]\\ &\le\zeta_k^\top\mathrm{J}_k^\top\big[\mathrm{I}-\mathrm{K}_{k+1}\mathrm{C}_{k+1}\big]^\top\Pi_{k+1}\big[\mathrm{I}-\mathrm{K}_{k+1}\mathrm{C}_{k+1}\big]\mathrm{J}_k\zeta_k\\ &\quad+r_k^\top\Pi_{k+1}\Big(2\big[\mathrm{I}-\mathrm{K}_{k+1}\mathrm{C}_{k+1}\big]\,\mathrm{J}_k\zeta_k+r_k\Big)\\ &\quad+2s_k^\top\Pi_{k+1}\Big(\big[\mathrm{I}-\mathrm{K}_{k+1}\mathrm{C}_{k+1}\big]\,\mathrm{J}_k\zeta_k+r_k\Big)\\ &\quad+s_k^\top\Pi_{k+1}s_k\end{aligned} \tag{A.5}$$

Taking the conditional expectation, $\mathbb{E}\big[V_{k+1}(e_{k+1})\,\big|\,e_k\big]$, the term

$$\begin{aligned}&\mathbb{E}\Big[2s_k^\top\Pi_{k+1}\Big(\big[\mathrm{I}-\mathrm{K}_{k+1}\mathrm{C}_{k+1}\big]\,\mathrm{J}_k\zeta_k+r_k\Big)\Big)\Big|\,e_k\Big]\\ &=2\mathbb{E}\big[s_k^\top\,|\,e_k\big]\,\mathbb{E}\Big[\Pi_{k+1}\Big(\big[\mathrm{I}-\mathrm{K}_{k+1}\mathrm{C}_{k+1}\big]\,\mathrm{J}_k\zeta_k+r_k\Big)\Big|\,e_k\Big]\end{aligned}$$

vanishes due to the fact that $\Pi_{k+1}(\,[\,\mathrm{I}-\mathrm{K}_{k+1}\mathrm{C}_{k+1}]\,\mathrm{J}_k\zeta_k+r_k)$ and ζ_k are independent of the noise term $s_k(\,w_k,v_{k+1}\,)$.

Applying *Lemma 1,2,3* on (A.5), we get

$$\begin{aligned}&\mathbb{E}\big[V_{k+1}(e_{k+1})\,\big|\,e_k\big]-V_k(e_k)\\ &\le\;-\beta V_k(e_k)+\kappa_{nonl_1}(\|e_k\|)+\kappa_{nonl_2}(\|e_k\|)\delta_w\\ &\quad+\kappa_{nonl_w}\delta_w^2+\kappa_{noise_w}\delta_w+\kappa_{noise_v}\delta_v\end{aligned} \tag{A.6}$$

Let $\|e_k\|\le\epsilon$ be the solution such that

$$\kappa_{nonl_1}(\|e_k\|)+\kappa_{nonl_2}(\|e_k\|)\delta_w \;\le\; \frac{\beta}{\overline{p}}\|e_k\|^2 \;\le\; \beta V_k(e_k)$$

where the second inequality follows from (A.4).

Then (A.6) becomes

$$\mathbb{E}\big[V_{k+1}(e_{k+1})\,\big|\,e_k\big]-V_k(e_k) \;\le\mu-\alpha V_k(e_k)$$

with $\mu=\kappa_{nonl_w}\delta_w^2+\kappa_{noise_w}\delta_w+\kappa_{noise_v}\delta_v$.

Finally, if there exist some positive constants ϵ, δ_w and δ_v such that (32) and (33) holds, together with (A.4), the conditions in (Reif et al., 1999, Lemma 2.1) is fulfilled. Hence, we proved that e_k is exponentially bounded in mean square and bounded with probability one. Then from (29), the same boundedness applies to ξ_k.